Predicting memapsin 2 (β-secretase) hydrolytic activity

Xiaoman Li,[1,2] Huang Bo,[3] Xuejun C. Zhang,[3] Jean A. Hartsuck,[1] and Jordan Tang[1,2]*

[1]Protein Studies Program, Oklahoma Medical Research Foundation, Oklahoma City, Oklahoma 73104

[2]Department of Biochemistry and Molecular Biology, University of Oklahoma Health Sciences Center, Oklahoma City, Oklahoma

[3]Institute of Biophysics, Chinese Academy of Sciences, Beijing 100101, China

Received 12 July 2010; Accepted 3 September 2010
DOI: 10.1002/pro.502
Published online 17 September 2010 proteinscience.org

Abstract: Memapsin 2 (BACE1, β-secretase), a membrane aspartic protease, functions in the cleavage of brain β-amyloid precursor protein (APP) leading to the production of β-amyloid. Because the excess level of β-amyloid in the brain is a leading factor in Alzheimer's disease (AD), memapsin 2 is a major therapeutic target for inhibitor drugs. The substrate-binding cleft of memapsin 2 accommodates 12 subsite residues, from P_8 to P_4'. We have determined the hydrolytic preference as relative k_{cat}/K_M (preference constant) in all 12 subsites and used these data to establish a predictive algorithm for substrate hydrolytic efficiency. Using the sequences from 12 reported memapsin 2 protein substrates, the predicted and experimentally determined preference constants have an excellent correlation coefficient of 0.97. The predictive model indicates that the hydrolytic preference of memapsin 2 is determined mainly by the interaction with six subsites (from P_4 to P_2'), a conclusion supported by the crystal structure *B*-factors calculated for the various residues of transition-state analogs bound to different memapsin 2 subsites. The algorithm also predicted that the replacement of the P_3, P_2, and P_1 subsites of APP from Val, Lys, and Met, respectively, to Ile, Asp, and Phe, respectively, (APP_{IDF}) would result in a highest hydrolytic rate for β-amyloid-generating APP variants. Because more β-amyloid was produced from cells expressing APP_{IDF} than those expressing APP with Swedish mutations, this designed APP variant may be useful in new memapsin 2 substrates or transgenic mice for AD studies.

Keywords: memapsin 2; BACE1; β-secretase; subsite specificity; activity prediction; β-amyloid; Alzheimer's disease

Introduction

Memapsin 2 (BACE1, β-secretase) is a membrane-anchored aspartic protease. Although this enzyme is ubiquitously present in many mammalian organs, its functions in the brain are best studied. One of the most important physiological functions of memapsin 2 is the cleavage of a brain membrane protein β-amyloid precursor protein (APP). The hydrolytic product of APP C-terminal fragment is cleaved again by γ-secretase to generate β-amyloid peptide (Aβ). Aβ has been shown to downregulate the synaptic activity in neurons.[1,2] Also, memapsin 2-produced APP N-terminal fragment is involved in the trimming of neurons and axons in the brain.[3] However, because excess levels of brain Aβ are intimately related to the pathogenesis of Alzheimer's disease (AD),[4] there has been intensive effort to develop inhibitor drugs against memapsin 2.[5] Important to such effort is the detailed knowledge on the specificity preference of this protease. In addition, there has been interest in

Abbreviations: Aβ, β-amyloid peptide; APP, β-amyloid precursor protein; APP_{SW}, APP with Swedish mutations; APP_{WT}, wild-type APP.

Additional Supporting Information may be found in the online version of this article.

Grant sponsor: NIH; Grant number: AG18933.

*Correspondence to: Jordan Tang, Protein Studies Program, Oklahoma Medical Research Foundation, 825, NE 13th Street, Oklahoma City, OK 73104. E-mail: jordan-tang@omrf.org

other possible physiological functions of memapsin 2 that need to be taken into consideration when developing inhibitors. The protease is known to be involved in the processing of neuregulin 1 during neuronal myelination in prenatal mice.[6,7] Other proteins processed by memapsin 2 include the beta-subunits of voltage-gated sodium channels (VGSC-βs),[8–10] alpha 2,6-sialyltransferase I (ST6GalI),[11] P-selectin glycoprotein ligand-1 (PSGL-1),[12] interleukin-1 receptor II (IL-IR2),[13] low-density lipoprotein receptor-related protein (LRP),[14] and amyloid-beta precursor-like proteins (APLPs).[15–17] The physiological significance of most of these cleavages is not clear, and only some of the memapsin 2 cleavage sites on these proteins have been determined. These studies have mostly been done in cells overexpressing potential substrate proteins that may lead to the enhanced cleavage of some nonphysiological substrates from their increased availability or distorted localization in subcellular compartments. Also, in cellular or *in vivo* experiments, memapsin 2 cleavage sites may be subjected to additional proteolysis by other cellular proteases, thus leading to the erroneous identification of memapsin 2 processing site, such as the case of alpha 2,6-sialyltransferase.[11,18] For these reasons, a clear understanding of memapsin 2 specificity with the ability to predict its activity toward different potential cleavage sites would be of assistance to the studies of physiological functions of this protease.

The polypeptide chain of memapsin 2 comprises a N-terminal ectocatalytic domain, a transmembrane domain, and a C-terminal cytosolic domain.[19] The catalytic domain is homologous to aspartic proteases of the pepsin superfamily in both the amino acid sequence[19] and in tertiary structure.[20] The activity of memapsin 2 is optimal near pH 4,[21] as is consistent with its function primarily within endosomal vesicles. The crystal structure of the catalytic domain shows that, like other aspartic proteases, memapsin 2 has a long substrate-binding cleft between the N- and C-terminal lobes that occupies nearly the entire width of the molecule.[20] The binding positions of transition-state analogs in the protease indicate that the substrate-binding cleft can accommodate 11–12 residues, with seven to eight residues at the N-terminus side (subsites P_8–P_1) and four at the C-terminal side (subsites P_1'–P_4').[20,22] We reported the residue preferences on 19 amino acids in eight memapsin 2 subsites, from S_4 to S_4', which are the subsites commonly present in aspartic proteases.[23] We also reported that memapsin 2 possesses three to four additional subsites and determined preferences in three of these sites, S_7, S_6, and S_5.[24] These data, determined as relative k_{cat}/K_M, which defines the relative efficiency of peptide bonds hydrolyzed by memapsin 2, established that this protease has a somewhat broad specificity in all subsites. Because these data represent the most complete specificity information of a nonstringent aspartic protease in kinetic constants, we asked if the contribution of different subsites to the determination of substrate cleavage sites can be expressed in quantitative terms and can be further developed as a predictive model for the probability of cleavage sites in any peptide substrate. Here, we describe an empirical model to quantitate the subsite contributions and predict the likelihood of cleavage of a peptide by memapsin 2.

Results

Complete residue preference on subsites P_5–P_8

To assess the contribution of all subsites on memapsin 2 catalysis, we need a complete set of subsite specificity data. Although the residue preferences for eight subsites, from P_4 to P_4', are complete,[23] only preliminary specificity data are available on four later discovered subsites P_5 to P_8.[24] Thus, the first task was to determine the complete residue preference in these four subsites using the same strategy as previously described.[23] Briefly, the initial cleavage rates of peptide substrates in a mixture by memapsin 2 were determined using ESI-TOF mass spectrometry. The relative rates under the experimental conditions were proportional to the relative k_{cat}/K_M (preference index) values.[25] Thus, peptide substrates differing from one another only by residues in a single subsite yielded relative preference for these residues. Preference index values for residues in subsites P_8, P_7, P_6, and P_5 are shown in Figure 1(A). Among these four subsites, amino acids in P_6 have the most effect on the substrate hydrolysis and tryptophan (W) and phenylalanine (F) are most favored. In the other three subsites, the differences among the residues are less noticeable. We observed that basic amino acids are generally unfavorable in at least three subsites, P_5, P_6, and P_7. Although there is a general agreement between the current data and the previous preliminary data,[24] the preference index values for tryptophan and basic amino acids were significantly different. For this reason, we used the stable-isotope-assisted MALDI-TOF mass spectrometry for better accuracy of the kinetic results. In the experimental design [Fig. 1(B)], peptides (P_6-1, P_7-1, and P_8-1) containing mixed amino acids at subsite to be tested were labeled with either *N*-acetoxy-D_0-succinimide or *N*-acetoxy-D_3-succinimide.[26] The D_3-acelyated peptides were subjected to memapsin 2 hydrolysis and mixed with equal amount of D_0-acelyated-modified same peptide. The two isotopes in each sample were determined in MALDI-TOF mass spectrometer. The D_3 data represent the hydrolytic rates, and the D_0 data serve as an internal standard. The relative hydrolytic rates, which represent the relative k_{cat}/K_M values[25] of P_6, P_7, or P_8, are shown in Figure 1(C). The isotope-MALDI-TOF study initially included P_5, but data from this

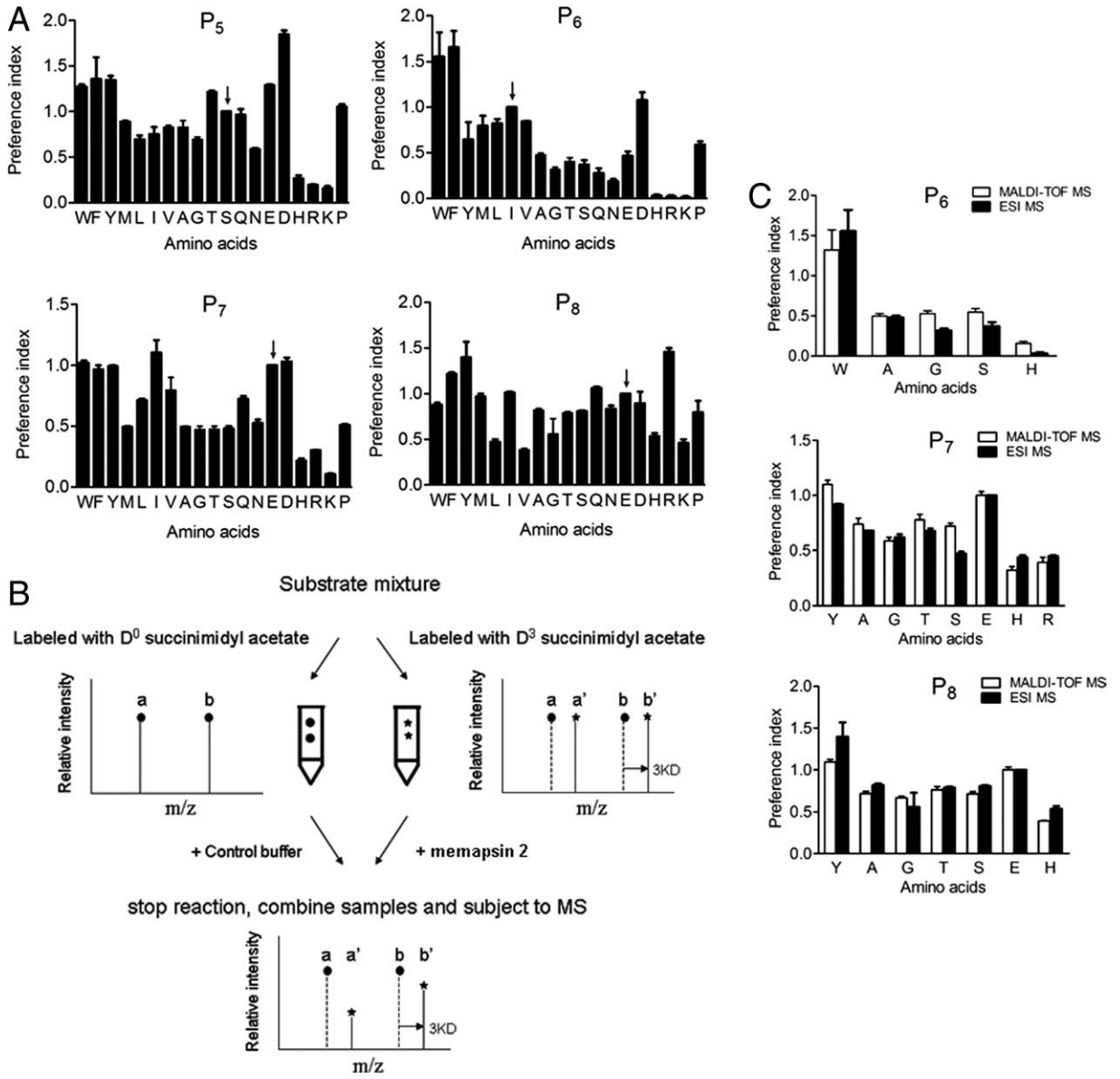

Figure 1. Preference of amino acid residues in the upstream subsites of memapsin 2 substrates. The preference index (see Materials and Methods) was calculated from the relative initial hydrolytic rates of the mixed substrates and is proportional to the relative k_{cat}/K_M. Amino acids (single-letter code) appear in the substrate template sequence at the position designated in each panel (P_n). The arrows indicate the residues found in native APP. (a) Complete amino acid residue preference for four subsites (S_5–S_8) derived by competitive hydrolysis assay from peptide mixture P_5–P_8 and ESI-TOF mass spectrometry. (b) Scheme of determination of subsite specificity by stable-isotope-assisted MALDI-TOF mass spectrometry. (c) Comparison of subsite specificity of upstream subsites, determined by competitive hydrolysis assay together with stable-isotope-assisted-MALDI-TOF mass spectrometry and ESI mass spectrometry using peptide mixtures containing representative substrates (P_6-1, P_7-1, and P_8-1).

subsite were not recovered. In spite of this loss, a comparison of data from P_6, P_7, or P_8 using these two methods clearly established that the relative preferences are in good agreement.

Comparison of the kinetics for peptides derived from memapsin 2 protein substrates

We studied the hydrolytic efficiency of APP and other reported substrates (Table I) by memapsin 2. Thirteen peptides of 12-residue each were synthesized based on the sequences around these cleavage sites so that each contained subsites from P_8 to P_4'. This group of peptides will be referred to as the "substrate peptide set." One of the peptides, VGSC-β2, was used for steady-state kinetic analysis for memapsin 2 hydrolysis resulting in k_{cat} and K_M values of 0.525 min^{-1} and 36.4 μM, respectively. The relative k_{cat}/K_M values of other 12 peptides were determined from their relative initial hydrolytic rates to that of VGSC-β2 peptide in substrate mixtures, under the condition $[S] << K_M$.[25] Wild-type APP (APP_{WT}), alpha 2,6-sialyltransferase I (ST6GalI), and IL-1R2 are substrates with low k_{cat}/K_M values in the range of 1–5 s^{-1} M^{-1} (Table I).

Table I. *Comparison of Sequence and Kinetic Properties of Different Memapsin 2 Substrates*

	Sequence													Cleavage site from membrane		Relative k_{cat}/K_M[b]	
Substrate[a]	P_8	P_7	P_6	P_5	P_4	P_3	P_2	P_1	*[c]	P'_1	P'_2	P'_3	P'_4	(a.a.)	k_{cat}/K_M (s^{-1} M^{-1})	Observed value	Calculated value
(1) APP_{WT}	E	E	I	S	E	V	K	M		D	A	E	F	29	1.02 ± 0.05	0.21	0.21
(2) APP_{SW}	E	E	I	S	E	V	N	L		D	A	E	F	29	486.55 ± 82.2	100	100
(3) VGSC-β1	S	V	V	K	K	I	H	L		E	V	V	D	16	0.30 ± 0.02	0.06	0.09
(4) VGSC-β2	R	G	H	G	K	I	Y	L		Q	V	L	L	13	24.30 ± 2.38	4.99	5.04
(5) VGSC-β3	N	V	S	R	E	F	E	F		E	A	H	R	31	0.33 ± 0.13	0.07	0.06
(6) VGSC-β4	N	N	S	A	T	I	F	L		Q	V	V	D	12	695.88 ± 97.93	143.02	99.42
(7) ST6GalI	S	D	Y	E	A	L	T	L		Q	A	K	E	11	1.85 ± 0.37	0.38	0.34
(8) IL-IR2	V	V	H	N	T	L	S	F		Q	T	L	R	15	4.00 ± 0.14	0.82	12.99
(9) NRG1	Y	K	H	L	G	I	E	F		M	E	A	E	10	41.39 ± 7.74	8.51	39.79
(10) NRG3	T	D	H	L	G	I	E	F		M	E	S	E	10	72.07 ± 9.87	14.81	39.79
(11) PSGL-1	I	P	M	A	A	S	N	L		S	V	N	Y	17	0.48 ± 0.02	0.10	0.11
(12) APP_{E11}	E	F	R	H	D	S	G	Y		E	V	H	H	19	0.02 ± 0.01	0.004	3.9×10^{-6}
(13) APP_{OK1}	Y	I	W	D	E	I	D	L		M	V	L	D	29	1760.59 ± 124.52	361.85	722.24

[a] (1)APPWT represents wild-type APP. (2) APPSW represents Swedish APP. (3)–(6) VGSC-β1, β2, β3, and β4 represent β1–β4 subunits of voltage-gated sodium channels. (7) ST6GalI represents α-2,6-sialyltransferase I. (8) IL-IR2 represents interleukin-1 receptor 2. (9) NRG1 represents neuregulin 1. (10) NRG3 represents neuregulin 3. (11) PSGL-1 represents P-selectin glycoprotein ligand-1. (12) APP_{E11} represents memapsin 2 alternative cleavage site on APP. (13) APP_{OK1} is not a natural substrate and synthesized by choosing the most favorable amino acid from each subsite according to the subsite specificity data [Ref. 23 and Fig. 1(A)].

[b] Relative k_{cat}/K_M of APP_{SW} is arbitrarily assigned as 100, and the relative k_{cat}/K_M values of other substrates are normalized to APP_{SW}.

[c] denotes the cleavage site.

Four peptides, β1 and β3 subunit of voltage-gated sodium channel (VGSC-β1, VGSC-β3), PSGL-1, and the peptide derived from the secondary cleavage site of APP (APP_{E11}), showed even lower cleavage efficiency with k_{cat}/K_M values of less than 0.5 s^{-1} M^{-1}. Three peptides are significantly better substrates than APP_{WT}. The k_{cat}/K_M values of voltage-gated sodium channel, subunit 2 (VGSC-β2), neuregulin 1 (NRG1), and neuregulin 3 (NRG3) are between 24 and 75 s^{-1} M^{-1}. The best natural substrate is voltage-gated sodium channel, subunit 4 (VGSC-β4), with a k_{cat}/K_M value of almost 700 s^{-1} M^{-1} compared with the k_{cat}/K_M value of the Swedish mutant of APP (APP_{SW}) value of 487 s^{-1} M^{-1}. The peptide APP_{OK1}, designed by choosing the most favorable amino acid from each subsite according to the subsite specificity data [Ref. 23 and Fig. 1(A)], shows a highest k_{cat}/K_M among all substrates, with a value of 1761 s^{-1} M^{-1}. These results show that memapsin 2 hydrolyzes the substrate peptide set with a wide range of efficiency.

An algorithm for memapsin 2 catalytic specificity

Information on the complete subsite specificity and kinetic data from substrate peptide set permitted us to address the question of whether these data can generate a quantitative model to assess the catalytic efficiency of potential memapsin 2 cleavage sites. We used the data for the substrate peptide set as a learning set to build and test an algorithm for relating the experimentally determined relative k_{cat}/K_M values to the calculated cleavage efficiency values. The agreement between these two sets of values served to evaluate the competence of the model. In developing the algorithm, we assumed that all the side chains of the substrate are equal in accessibility by memapsin 2, and that the contribution of each side chain in cleavage efficiency is independent of other side chains. Also, we assumed that the contribution of each subsite to the cleavage efficiency is different from that of the other subsites, as suggested from the different stringency on residue specificity in different subsites. These assumptions led us to an equation similar to a weighted geometric mean of the various specificities because we expected the effects of the individual subsites to be multiplicative. The resulting equation is as follows:

$$Q = \mathrm{Exp}(\sum w_i \ln a_i),$$

where Q is the arbitrary value for memapsin 2 cleavage efficiency, a_i is the experimentally determined relative k_{cat}/K_M value (Supporting Information Table I) of the amino acid at P_i subsite position, and w_i is the weighting factor of that particular subsite. The w_i values were determined by nonlinear regression to achieve a maximal correlation coefficient value between the Q values and the actual kinetic data of the substrate peptide set. The optimized w_i values are shown in Table II, and corresponding Q values for the substrate peptide set are

Table II. *Weighting Factor for P_4 to P_2' Subsite*

W_4	W_3	W_2	W_1	W_1'	W_2'
0.89	3.50	1.02	6.26	0.38	1.09

shown in Table I. During the optimization process, we found that only six subsites, P_4–P_2', significantly influenced the calculated Q values; thus, the outside subsites were dropped from the further calculations. A plot of the Q values and the relative k_{cat}/K_M data showed a linear correlation (Fig. 2) with a correlation coefficient of 0.97. The correlation of the observed and calculated data in Figure 2 was further validated by a "leave-one-out cross validation," which is one type of K-fold cross validation. Under this test, the mean correlation coefficient was 0.96 ± 0.012. The closeness of the mean correlation coefficient to the original value and the narrow deviation of the mean clearly established the validity of the algorithm.

To test this algorithm, we selected a 15-residue peptide cerebellin (GSAKVAFSAIRSTNH), which is not a natural substrate of memapsin 2. This peptide was chosen because it is small enough to be unbiased in specific tertiary structures yet contains enough residues to be recognized by multiple subsites of memapsin 2. The application of the algorithm predicted a distinct cleavage site at the Phe-Ser bond (Table III) with a k_{cat}/K_M value of 0.24 s^{-1} M^{-1}. Analysis of hydrolytic products of cerebellin by memapsin 2 in MALD-TOF mass spectrometry showed essentially two products with masses of 679.18 and 885.24 Da (Fig. 3), which are assigned to the fragment GSAKVAF and SAIRSTNH, the N-terminal and C-terminal products generated from the predicted cleavage site, respectively. The k_{cat}/K_M value determined for the cleavage of this site was 0.14 s^{-1} M^{-1}. Overall, these results confirmed the predicted cleavage site using the algorithm.

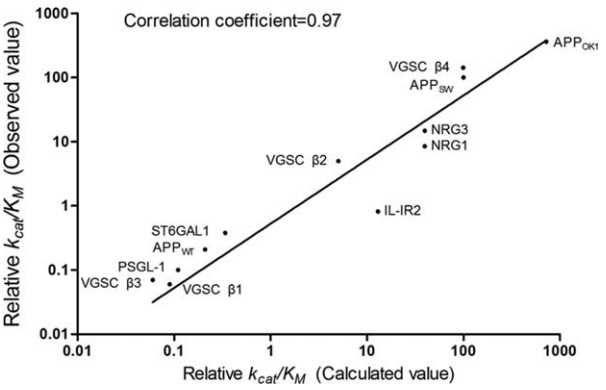

Figure 2. Correlation of the calculated and observed relative k_{cat}/K_M values of different substrates. The calculated relative k_{cat}/K_M of different substrates is plotted to the relative k_{cat}/K_M of different substrates determined by experiments (the relative k_{cat}/K_M of peptide derived from Swedish APP is arbitrarily assigned as 100; the relative k_{cat}/K_M of other substrates is determined by normalizing to Swedish APP). Logarithmic scale is used for X and Y axes. The correlation coefficient for the predicted data to experimental data is 0.97.

Table III. *Comparison of Possible Cleavage Sites in Cerebellin*

Possible cleavage sites[a]	Possible peptides mass after cleavage		Predicted relative k_{cat}/K_M[b]
GSAKVAFSAIR* STNH	1106.63	458.20	1.34×10^{-15}
GSAKVAFSAI* RSTNH	950.53	614.30	1.80×10^{-15}
GSAKVAFSA* IRSTNH	837.45	727.38	2.75×10^{-16}
GSAKVAFS* AIRSTNH	766.41	798.42	3.22×10^{-8}
GSAKVAF* SAIRSTNH	679.38	885.45	0.24
GSAKVA* FSAIRSTNH	532.31	1032.52	2.34×10^{-15}
GSAKV* AFSAIRSTNH	461.27	1103.56	1.74×10^{-14}
GSAK* VAFSAIR STNH	362.20	1202.63	1.30×10^{-14}

[a] Amino acid residues are shown in one-letter code;
* represents the possible cleavage site.
[b] Relative k_{cat}/K_M of APPsw is arbitrarily assigned as 100, and the predicted relative k_{cat}/K_M values of different possible cleavage sites are normalized to APPsw.

Determine B*-factor values of residues in memapsin 2 subsites*

Because the efficiency of substrate hydrolysis is related to the transition-state binding, it was of interest to obtain physical data on binding intensity of inhibitor residues in the subsites of memapsin 2 for comparison with the kinetic data of the subsites. Several crystal structures of memapsin 2 complex to inhibitors are available in the database. Of these, five inhibitors are transition-state analogs in which the scissile peptide bonds were replaced by a transition-state isostere. We reasoned that the B-factor (crystallographic temperature factor) of the inhibitor side chains, which is an indicator for the motion or variability in the structure, should be inversely related to the transition-state binding intensity of these residues and may also mirror the parameters determined by enzyme kinetics.

The normalized B-factor values of each side chain in the five inhibitors were determined and shown in Figure 4. There is a significant increase in the side chain B-factors for positions P_3' and P_4' when compared with the other inhibitor subsites. This is consistent with our observation that subsites P_3' and P_4' do not have significant influence on the calculated k_{cat}/K_M for any peptide. The correlation of the normalized reciprocal weighting factors (Fig. 4, heavy line) with the aggregate of the B-factors is good except for position P_1'. The reciprocal of the weighting factor for subsite P_1' developed for the algorithm is much higher than the other subsite weights and higher than the comparable B-factors. Consequently, in the predictive calculations, subsite

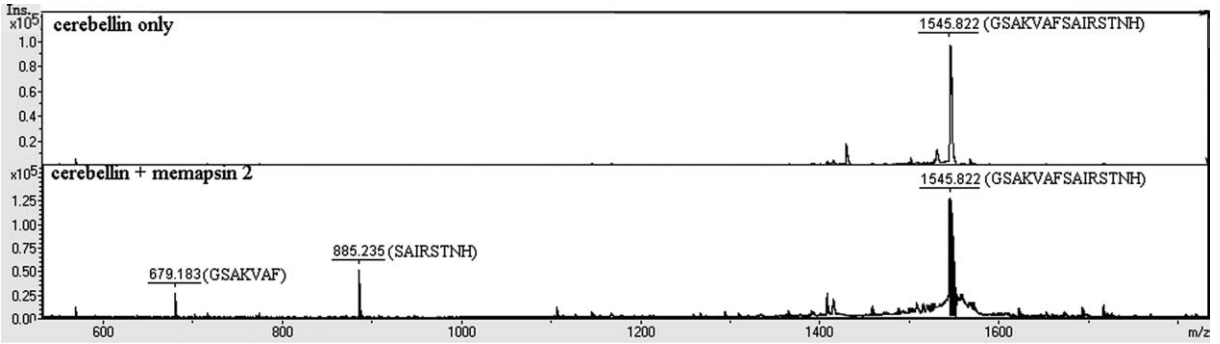

Figure 3. Hydrolysis of cerebellin by memapsin 2. Upper panel: cerebellin only. Lower panel: cerebellin digested with memapsin 2. After digestion, two products appear with masses of 679.18 and 885.24 Da, which are assigned to the fragment GSAKVAF and SAIRSTNH, the N-terminal and C-terminal products generated from the predicted cleavage site, respectively.

P_1' has less influence on the k_{cat}/K_M of a substrate than do the other subsites.

Design an APP mutant for maximal production of amyloid-beta

The results above show that the mutations of P_2 Lys and P_1 Met in APP_{WT} to P_2 Asn and P_1 Leu, respectively (APP_{SW}), increased the k_{cat}/K_M value by 477-fold (Table I). Because the P′ residues are not changed, both APP_{WT} and APP_{SW} produce the same amyloid-β (Aβ) peptides, and this greatly enhanced production leads to an early onset of AD in APP_{SW} mutation. With the availability of the algorithm described above, it was of interest to design a highly efficient memapsin 2 cleaving APP mutant with new residue mutations only on the P subsites, thus it would still produce the native Aβ. The algorithm predicted that the mutation of residues in APP_{WT} from P_3 Val, P_2 Lys, and P_1 Met to P_3 Ile, P_2 Asp, and P_1 Phe, respectively (APP_{IDF}), would increase the k_{cat}/K_M value by about 849-fold, about 1.7 times higher than that for APP_{SW}. To investigate the production of Aβ by APP_{IDF} in the cells, we mutated

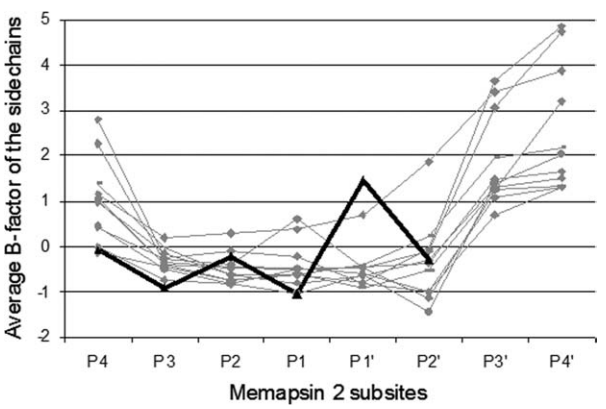

Figure 4. Comparison of normalized *B*-factors of inhibitor side chains with the reciprocal weighting factors for the subsites P_4 to P_4'. Normalized *B*-factors of several bound inhibitor side chains are shown in gray. The black line is the reciprocal of the weighting factor calculated in this work (Table II). The reciprocal weighting factor has been normalized to the aggregate of the *B*-factors.

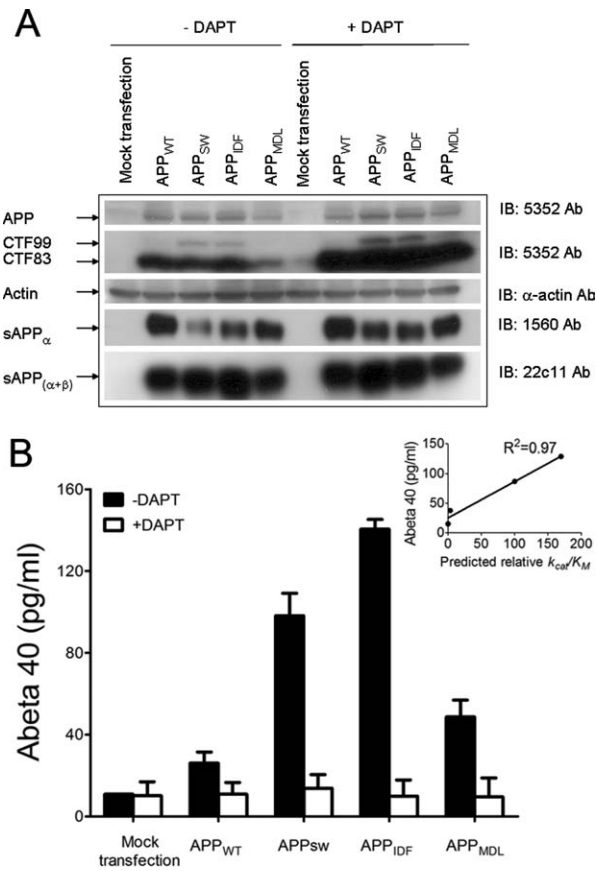

Figure 5. Processing of APP variants by memapsin 2. (a) CAD cell line was transfected with each APP construct followed by Western analysis of cell lysates and conditioned medium. The 5352 antibody was used for detecting full-length APP, CTF 99, and CTF 83. sAPPα was detected by Ab 1560. The 22C11 antibody is used for detecting sAPP (sAPPα + sAPPβ). (b) Quantitation of soluble amyloid peptides was performed by ELISA. The fold increase of different APP mutants compared with APP_{WT} is shown in the inset.

Table IV. *Comparison of Possible Cleavage Sites in APLP1, APLP2, mPGES-2, and ST6GalI by Memapsin 2*

Protein[a]	Sequence and possible cleavage site		Predicted relative k_{cat}/K_M[b]	Distance from membrane
APLP2	1 2 3 4 5 6			
	▼ ▼ ▼ ▼ ▼ ▼	1.	0.23	40
	KVDENM VIDETL DVKEM IF NAERVGGL EEERESVGPL REDFSLSSS	2.	0.18	34
		3.	1×10^{-3}	29
		4.	4×10^{-3}	27
		5.	7×10^{-7}	19
		6.	1×10^{-7}	9
APLP1	7 8 9 10 11 12			
	▼ ▼ ▼ ▼ ▼ ▼	7.	1×10^{-6}	40
	PEKEKM NPL EQY ERKVNASVPRGF PF HSSEIQRDEL APAGTGVSRE	8.	6×10^{-9}	37
		9.	3×10^{-6}	34
		10.	3×10^{-9}	22
		11.	3×10^{-5}	20
		12.	5×10^{-5}	10
mPGES-2	13 14 15 16			
	▼ ▼ ▼ ▼	13.	1×10^{-4}	[c]
	HLRAQDL HA ERSAAQL SL SS	14.	6×10^{-14}	[c]
		15.	0.08	[c]
		16.	36	[c]
ST6GalI	17 18			
	▼ ▼	17.	0.3	11
	SDYEALTL QAK EFQ	18.	1×10^{-16}	14

[a] APLP1 and APLP2 represent amyloid-beta (A4) precursor-like protein 1 and 2; mPGES-2 represents membrane-associated prostaglandin E2 synthase-2; ST6GALI represents α-2,6-sialyltransferase I.
[b] Relative k_{cat}/K_M of APPsw is arbitrarily assigned as 100, and the predicted relative k_{cat}/K_M values of different possible cleavage sites are normalized to APPsw.
[c] mPGES-2 is a membrane-associated protein, while all the other proteins in this table are transmembrane proteins.

these three residues in APP_{WT}, transfected the expression vector of APP_{IDF} into mouse neuronal CAD cells, and determined degradation products of APP. Another APP variant with P_3 Met, P_2 Asp, and P_1 Leu, APP_{MDL}, has a predicted k_{cat}/K_M value about 18 times of that for APP_{WT}, was also studied as comparison.

The Western blot for APP indicated that the expression levels of APP_{WT}, APP_{SW}, APP_{IDF}, and APP_{MDL} were about the same [Fig. 5(A), top panel]. APP_{SW} cells produced about fourfold of Aβ than did APP_{WT} cells, and the cells expressing APP_{IDF} produced about 40% more Aβ than APP_{SW} cells [Fig. 5(B)]. Aβ produced by APP_{MDL} was between APP_{WT} and APP_{SW}. A plot of Aβ and predicted relative k_{cat}/K_M values of four APP clones showed a good linear correlation [Fig. 5(B), inset]. APP_{IDF} and APP_{SW} cells were similar in cellular processing characteristics. Both revealed a detectable accumulation of APP C-terminal fragment of 99 residues (CTF99), the direct product of memapsin 2 cleavage, which is not visible in APP_{WT} cells [Fig. 5(A), second panel, left lanes]. CTF99 is increased in both APP_{IDF} and APP_{SW} cells when γ-secretase inhibitor DAPT slowed its degradation [Fig. 5(A), second line, right lanes]. As expected, APP ectodomain fragment from α-secretase cleavage, sAPPα, decreased in both APP_{IDF} and APP_{SW} cells when compared with that in APP_{WT} cells [Fig. 5(A), fourth panel]. Taken together, the above results indicate that APP_{IDF} produces a higher level of Aβ than that for APP_{SW} in a neuronal cell line and its degradation pathways are mediated through three secretases.

Discussion

The determination of subsite specificity of aspartic proteases usually requires many kinetic analyses. Because most of these proteases have eight or more subsites and have nonstringent specificity, very few subsite specificity of these enzymes have been completely determined. For memapsin 2, the residue preference, expressed as relative k_{cat}/K_M values, is now known for 12 subsites, from P_8 to P_4'. Therefore, these data on memapsin 2 represent the first complete kinetic assessment of the subsite preference of an aspartic protease, which offers a new opportunity for dissecting the influence of subsite residues on hydrolytic activity and establishing an algorithm for predicting memapsin 2 activity. The general applicability of the algorithm is supported by a good correlation coefficient between the

predicted and experimentally determined preference constants by the result in a test substrate cerebellin.

We have used the algorithm to predict memapsin 2 cleavage activity of several proteins of interest. First, four peptides containing sequences from the reported memapsin 2 substrates (Table I, Nos. 3, 5, 11, and 12) were very poor substrates. The fact that the relative k_{cat}/K_M value of APP_{WT} near the values for these four peptides seems to suggest that the functions of memapsin 2 *in vivo* do not require substrates with highly favorable bonds, as both enzyme and substrates are membrane anchored so the substrate is well positioned to be cleaved. This line of argument is supported by our observation that the memapsin 2-cleaved bonds in these protein substrates are located in a region from 10 to 31 amino acid residues from the membrane (Table I). Our data also clearly show that subsite specificity is the main factor for cleavage efficiency, once the substrate is in the protease's effective range. For example, the cleavage positions of APP_{WT} and APP_{SW} are both 29 residues from the membrane yet differ in hydrolytic efficiency by near 500 times. Another interesting point related to the above discussion is that memapsin 2 cleavage sites in APP_{WT} (Table I, number 1) and APP_{E11} (Table I, number 12) are present on the same APP molecule, thus should be competing cleavage sites. The cleavage of $APPE_{11}$ produces a shorter peptide, Glu11-Aβ, after the γ-secretase cleavage.[27] Based on the relative k_{cat}/K_M of these two sites, the production ratio of Aβ to Glu11-Aβ would be about 50 to 1 from APP_{WT}. However, in cells producing APP_{SW}, this ratio would be about 25,000 to 1, greatly diminishing the production of Glu11-Aβ and its possible physiological roles.

Second, two APP homologs, APLP1 and APLP2, are known to be cleaved by memapsin 2.[15–17] However, the actual cleavage sites have not been determined. We have used the algorithm to predict the potential memapsin 2 cleavage sites in the region of 55 residues adjacent to the membrane in the ectodomains of these proteins. For APLP2, two potential cleavage sites (sites 1 and 2 in Table IV) were predicted at 40 and 34 residues from the membrane. The estimated cleavage efficiency is about the same as that of the β-site of APP_{WT} (Table I). Sites 3 and 4 (Table IV) are about 50 to 200 times lower than the values for sites 1 and 2. Thus, memapsin 2 cleavage of sites 3 and 4 seems less probably even though these sites are located in the effective cleavage range. For APLP1, the algorithm predicted no efficient cleavage site with the highest kinetic value is only 1/4000 in cleavage efficiency when compared with the β-site of APP_{WT} (Table IV). These results suggest that APLP1 is not an effective substrate of memapsin 2.

Third, prostaglandin E2 synthetase 2 has been reported to be cleaved by memapsin 2.[28] The proposed cleavage site, however, is extremely unfavorable (site 14, Table IV) and is unlikely to be significantly cleaved by memapsin 2. Two nearby sites (sites 15 and 16, Table IV) have much better values for cleavage preference and are more likely to be the probable sites for memapsin 2 processing. The usefulness of the current algorithm prediction is also illustrated in the case of memapsin 2 cleavage site in alpha 2,6-sialotransferase 1. The cleavage site initially reported (site 18, Table IV)[11] was three residues away from the actual cleavage site later determined (site 17, Table IV).[18] The predicted kinetic values (Table IV) show that site 17 is favorable and site 18 is extremely unfavorable for memapsin 2 cleavage.

The algorithm described here was developed based on the assumption that the recognition of each side chain by a protease subsite is independent and the peptide substrates have random conformation in solution. The very high correlation between the predicted preference constants (relative k_{cat}/K_M) and the actual data derived from *in vitro* experiments appears to support the assumption. *In vivo* substrates of memapsin 2 are proteins that conceivably may retain some conformation in the peptide strands near the cleavage sites and may differ from the *in vitro* rates. However, the fact that substrate analogs bind to the memapsin 2 active site in extended conformation argues for an extended, denatured state of the peptide strands at least locally near the cleavage sites. Such a "local denaturation" of the cleavage sites could be facilitated by the acidic environment inside of the endosomal vesicles where the majority of memapsin 2 activity is manifested.[29,30]

We observed an interesting correlation between the current algorithm and temperature (*B*-) factors of the side chains in the crystal structures of transition-state analog inhibitors complex to memapsin 2. In spite of limited residue variation in the inhibitors bound to the protease (see structures in Materials and Methods), there is a clear similarity in the normalized *B*-factors of the side chains and the inverse values of the weighting factors determined in this work (Fig. 4). The *B*-factor values in this case reflect the degree of freedom in the motion for the side chains and should be inversely related to the tightness of their binding in different subsite pockets. Because these inhibitors are transition-state analogs, the *B*-factor values of the individual subsites may reflect inversely their contributions to the transition-state binding during the catalysis and to the kinetic parameter k_{cat}. Although the weighting factors are empirically determined from the formulation of our algorithm, the similar trend of these two sets of values suggests that the weighting factors are influenced in large extent by the contribution of individual subsites to the overall k_{cat} of the substrates. We

noticed that the *B*-factor values for subsites P_3' and P_4' were much larger than those of the other subsites (Fig. 4). This is in agreement with the observation that the inclusion of these subsites in the calculation did not improve the outcome of the prediction of cleavage preference. As can be seen in Figure 4, the agreement between *B*-factor and weighting factor is poorest at subsite P_1'. Different computational schemes attempted did not produce an equally competent algorithm with a higher weighting factor for subsite P_1'. We tentatively suggest that this subsite may have other mechanistic roles in memapsin 2 catalysis, thus is not strictly related to the transition-state binding. In view of the excellent correlation coefficient for the experimental and prediction values (Fig. 2), we feel that the impact of this discrepancy on the overall ability of the algorithm to predict cleavage preference is relatively small.

The kinetic data on natural substrates of memapsin 2 offer an interesting range of hydrolytic efficiency of about 35,000-fold variation (Table I). The wild-type APP_{WT}, which is the best established physiological substrate of memapsin 2, is in fact among the substrates with relatively low hydrolytic efficiency by memapsin 2. APP_{IDF} and APP_{SW}, both generate native Aβ, increase the k_{cat}/K_M value by 849 and 479 times from that of APP_{WT}, respectively. These comparisons argue for the hypothesis that the structural mutations to attain the highest cleavage efficiency of APP as a memapsin 2 substrate have not been subjected to survival selection in evolution. This may be because other criteria, such as regulation of Aβ production, are more important criteria for evolutionary selection.

The design of APP_{IDF} further demonstrated the potential application of the algorithm model. The predicted hydrolytic efficiency of APP_{IDF} by memapsin 2 is 1.7-fold of that for APP_{SW}. In cellular experiments, we observed that the production of Aβ from APP_{IDF} up to 1.5-fold that from APP_{SW}. Up to now, APP_{SW} has been the APP mutant that produces the highest amount of Aβ and its sequence has been used in peptide substrates for memapsin 2 assays. APP_{SW} has also been used to produce a number of transgenic mouse strains[31,32] that manifest both brain amyloid plaques and loss of cognitive functions upon aging. These mouse strains are widely used as experimental models for AD in human. Our current results indicate that peptides containing APP_{IDF} would be more efficient substrates for memapsin 2 than those containing APP_{SW} sequences, and it would be of interest to study transgenic mouse strains with the APP_{IDF} mutations as animal models of AD. The probability of a clinical observation of an early onset of AD with APP_{IDF} mutations is probably very small because five mutations need to occur for the conversion of APP_{WT} to APP_{IDF}, when compared with the formation of APP_{SW} would need only two mutation steps.

Materials and Methods

Materials

α-Cyan-4 hydroxycinnamic acid, D_0- and D_6-form acetic anhydride, and *N*-hydroxysuccinimide were purchased from Sigma. Peptide (Des-Ser1)-cerebellin was purchased from Bachem (Bubendorf, Switzerland). All peptides derived from memapsin 2 potential substrates were synthesized by GenScript (Piscataway, NJ). The ectodomain of human memapsin 2 was expressed and purified as described previously.[20] Monoclonal anti-APP antibody 1560, MAB348 (22C11), and polyclonal anti-APP antibody 5352 were purchased from Millipore (Billerica, MA). Monoclonal anti-actin antibody was purchased from Abcam (Cambridge, MA).

Design of the defined substrate mixtures

Peptide sequence RK (P_{10})T(P_9)E(P_8)E (P_7)I(P_6)S (P_5)E(P_4)V(P_3)N(P_2)L(P_1)*D(P_1')A(P_2')E(P_3')F(P_4'), corresponding to the amino acid sequence of APP with Swedish mutation from P_{10} to P_4', was used to be a template to study residue preferences in substrate mixtures (* denotes the cleavage site). Four sets of separate substrate mixtures were synthesized by Synpep (Dublin, CA): RKTEEI-[X]-EVNL*DAEF, RKTEE-[X]-SEVNL*DAEF, RKTE-[X]-ISEVNL*DAEF, and RKT-[X]-EISEVNL*DAEF. These four sets contain residue mixture (represented by X) of 19 amino acids (cysteine is not included as it spontaneously forms disulfide in kinetic measurements and also in protein substrates cysteines are in disulfides, which are not cleaved by memapsin 2) at positions corresponding to P_5, P_6, P_7, and P_8, respectively. A peptide derived from APP_{SW}, RKTEEISEVNL*DAEF, was also added to each mixture to serve as an internal standard. Three additional sets of mixtures used previously[24] were also used here, RTEE-[X]-SEVNL*AAEF for the study of P_6 subsite, RTE-[X]-ISEVNL*AAEF for the study of P_7 subsite, and RT-[X]-EISEVNL*AAEF for the study of P_8 subsite (they will be referred to as peptide mixtures P_6-1, P_7-1, and P_8-1, respectively).

Kinetic analysis of subsite specificity using ESI-TOF mass spectrometry

Substrate mixtures were dissolved at 10 mg mL^{-1} in DMSO and were further diluted to 10 μM in 0.1*M* MOPS buffer (pH 4.0). The reactions were initiated by the addition of memapsin 2; aliquots were removed at time intervals and quenched by formic acid. Quantitative analysis was conducted by ESI LC/MS. The system was composed of an Agilent 1100 HPLC, a Clipeus 50 mm × 5 mm C-18 column, and a Bruker MicroTOF ESI-MS. Relative product formed per unit time was calculated similar as previously described.[23] A relative catalytic efficiency (k_{cat}/K_M) of 1.0 was assigned to the internal standard peptide, APP_{SW}. Therefore, the relative k_{cat}/K_M of any other substrate is determined by comparing its pseudo first-order

rates of cleavage to that of the APP_{SW} peptide. For convenience of discussion, the relative k_{cat}/K_M value is also referred to as "preference index."

Kinetic analysis of subsite specificity using stable isotope-assisted MALDI-TOF mass spectrometry

N-acetoxy-D_0 (D_3)-succinimide was synthesized from *N*-hydroxysuccinimide and D_0 (D_6)-form acetic anhydride as previously described.[26] Each of the peptide mixture (P_6-1, P_7-1, and P_8-1) was equally divided and incubated with either *N*-acetoxy-D_0-succinimide or *N*-acetoxy-D_3-succinimide in 25 m*M* ammonium bicarbonate, pH 7.5, for 3 h. D_0- or D_3-aceylated-modified peptide mixtures were individually diluted into 0.1*M* MOPS, pH 4.0, to obtain a final concentration of 6 μ*M*. At room temperature, an aliquot of memapsin 2 was added to the D_3-modified sample. At different time points, an aliquot sample was taken out, quenched by formic acid, and pooled with equal volume of the D_0-labeled sample. Samples of 0.5 μL were each combined with equal amount of saturated α-cyan-4 hydroxycinnamic acid matrix in 50% acetonitrile/0.1% TFA and subjected to Bruker Ultraflex MALDI-TOF mass spectrometer. Relative product formation was calculated as the ratio of the reduction of substrate's signal intensity by comparing the amount of D_3 to its reference D_0. The relative k_{cat}/K_M was calculated as described above.

Plasmid construction and mutagenesis

APP (770 isoform) was subcloned into pSecTag vector. Different mutations flanking the β-cleavage site (P_3–P_1) APP_{SW}, APP_{IDF}, and APP_{MDL} were generated by Stratagene QuikChange Site-Directed Mutagenesis Kit and individually confirmed by DNA sequencing.

Cell culture, transfection, and analysis of APP processing products

Mouse neuronal CAD cell line was cultured with DMEM/F12 media (Invitrogen, Carlsbad, CA). Transient transfections were performed using Roche Fugene HD according to the manufacture's instruction. Twenty-four hours after transfection, total cell lysate and cell media were collected. Aβ level in media was assayed by Aβ [$^{1–40}$] Human Fluorimetric ELISA Kit (Invitrogen). Conditioned media or total cell lysate from the transiently transfected cells were subjected to Western blot with antibody against full-length APP, APP's proteolytic products, and β-actin.

Calculation of B*-factors of residues in the subsites of memapsin 2-inhibitor complexes*

Crystal structures of memapsin 2-inhibitor complexes from PDB IDs 1FKN, 1M4H, 1XN3, 2ZHR, and 1XN2 were included in the ligand *B*-factor statistic analysis. The structures of the inhibitors are as follows: 1FKN, Glu-Val-Asn-Leu ψ Ala-Ala-Phe, where ψ represents transition-state isostere hydroxyethylene; 1M4H, Glu-Leu-Asp-Leu ψ Ala-Val-Glu-Phe; 1XN3, Lys-Thr-Glu-Glu-Ile-Ser-Val-Asn-Sta-Val-Ala-Glu-Phe, where Sta is statine; 2ZHR, Glu-Val-Asn-Leu ψ Ala-Glu-Phe; and1XN2, Trp-Trp-Ser-Glu-Val-Asn-Leu ψ Ala-Ala-Glu-Phe. For each protease–ligand complex in a crystallography asymmetric unit, residues of the peptide ligand were identified visually and assigned subsites from P_4 to P_4' accordingly. The average *B*-factor of each subsite was calculated for the side chain. Before comparing the average *B*-factors of each subsite from different crystal structures, a statistical normalization was performed with the following equation.

$$B_{\text{norm}} = \frac{B - \overline{B}}{\sqrt{\frac{1}{N}\sum_{i=1}^{N}(B_i - \overline{B})^2}},$$

where N is the number of all atoms from the refined structure of a given PDB file; $\overline{B}$ is the average *B*-factor of all main-chain atoms (which are supposed to be refined more reliably) from the same PDB file. B is the *B*-factor to be normalized; here, it is the average *B*-factor of a certain subsite. A value below zero indicates that this group of atoms is less mobile than the average *B*-factor of main-chain atoms, and a value above zero indicates that this group of atoms is more mobile than the average.

Acknowledgment

JT is the holder of the J. G. Puterbaugh Chair in Biomedical Research at the Oklahoma Medical Research Foundation.

References

1. Kamenetz F, Tomita T, Hsieh H, Seabrook G, Borchelt D, Iwatsubo T, Sisodia S, Malinow R (2003) APP processing and synaptic function. Neuron 37:925–937.
2. Lauren J, Gimbel DA, Nygaard HB, Gilbert JW, Strittmatter SM (2009) Cellular prion protein mediates impairment of synaptic plasticity by amyloid-beta oligomers. Nature 457:1128–1132.
3. Nikolaev A, McLaughlin T, O'Leary DD, Tessier-Lavigne M (2009) APP binds DR6 to trigger axon pruning and neuron death via distinct caspases. Nature 457: 981–989.
4. Selkoe DJ (1999) Translating cell biology into therapeutic advances in Alzheimer's disease. Nature 399: A23–A31.
5. Ghosh AK, Gemma S, Tang J (2008) Beta-secretase as a therapeutic target for Alzheimer's disease. Neurotherapeutics 5:399–408.
6. Willem M, Garratt AN, Novak B, Citron M, Kaufmann S, Rittger A, DeStrooper B, Saftig P, Birchmeier C, Haass C (2006) Control of peripheral nerve myelination by the beta-secretase BACE1. Science 314:664–666.
7. Hu X, Hicks CW, He W, Wong P, Macklin WB, Trapp BD, Yan R (2006) Bace1 modulates myelination in the central and peripheral nervous system. Nat Neurosci 9: 1520–1525.

8. Wong HK, Sakurai T, Oyama F, Kaneko K, Wada K, Miyazaki H, Kurosawa M, De Strooper B, Saftig P, Nukina N (2005) Beta subunits of voltage-gated sodium channels are novel substrates of beta-site amyloid precursor protein-cleaving enzyme (BACE1) and gamma-secretase. J Biol Chem 280:23009–23017.
9. Kim DY, Carey BW, Wang H, Ingano LA, Binshtok AM, Wertz MH, Pettingell WH, He P, Lee VM, Woolf CJ, Kovacs DM (2007) BACE1 regulates voltage-gated sodium channels and neuronal activity. Nat Cell Biol 9: 755–764.
10. Miyazaki H, Oyama F, Wong HK, Kaneko K, Sakurai T, Tamaoka A, Nukina N (2007) BACE1 modulates filopodia-like protrusions induced by sodium channel beta4 subunit. Biochem Biophys Res Commun 361:43–48.
11. Kitazume S, Tachida Y, Oka R, Shirotani K, Saido TC, Hashimoto Y (2001) Alzheimer's beta-secretase, beta-site amyloid precursor protein-cleaving enzyme, is responsible for cleavage secretion of a Golgi-resident sialyltransferase. Proc Natl Acad Sci USA 98:13554–13559.
12. Lichtenthaler SF, Dominguez DI, Westmeyer GG, Reiss K, Haass C, Saftig P, De Strooper B, Seed B (2003) The cell adhesion protein P-selectin glycoprotein ligand-1 is a substrate for the aspartyl protease BACE1. J Biol Chem 278:48713–48719.
13. Kuhn PH, Marjaux E, Imhof A, De Strooper B, Haass C, Lichtenthaler SF (2007) Regulated intramembrane proteolysis of the interleukin-1 receptor II by alpha-, beta-, and gamma-secretase. J Biol Chem 282:11982–11995.
14. von Arnim CA, Kinoshita A, Peltan ID, Tangredi MM, Herl L, Lee BM, Spoelgen R, Hshieh TT, Ranganathan S, Battey FD, Liu CX, Bacskai BJ, Sever S, Irizarry MC, Strickland DK, Hyman BT (2005) The low density lipoprotein receptor-related protein (LRP) is a novel beta-secretase (BACE1) substrate. J Biol Chem 280: 17777–17785.
15. Li Q, Sudhof TC (2004) Cleavage of amyloid-beta precursor protein and amyloid-beta precursor-like protein by BACE 1. J Biol Chem 279:10542–10550.
16. Pastorino L, Ikin AF, Lamprianou S, Vacaresse N, Revelli JP, Platt K, Paganetti P, Mathews PM, Harroch S, Buxbaum JD (2004) BACE (beta-secretase) modulates the processing of APLP2 in vivo. Mol Cell Neurosci 25: 642–649.
17. Walsh DM, Minogue AM, Sala Frigerio C, Fadeeva JV, Wasco W, Selkoe DJ (2007) The APP family of proteins: similarities and differences. Biochem Soc Trans 35: 416–420.
18. Kitazume S, Tachida Y, Oka R, Kotani N, Ogawa K, Suzuki M, Dohmae N, Takio K, Saido TC, Hashimoto Y (2003) Characterization of alpha 2,6-sialyltransferase cleavage by Alzheimer's beta-secretase (BACE1). J Biol Chem 278:14865–14871.
19. Lin X, Koelsch G, Wu S, Downs D, Dashti A, Tang J (2000) Human aspartic protease memapsin 2 cleaves the beta-secretase site of beta-amyloid precursor protein. Proc Natl Acad Sci USA 97:1456–1460.
20. Hong L, Koelsch G, Lin X, Wu S, Terzyan S, Ghosh AK, Zhang XC, Tang J (2000) Structure of the protease domain of memapsin 2 (beta-secretase) complexed with inhibitor. Science 290:150–153.
21. Ermolieff J, Loy JA, Koelsch G, Tang J (2000) Proteolytic activation of recombinant pro-memapsin 2 (pro-beta-secretase) studied with new fluorogenic substrates. Biochemistry 39:12450–12456.
22. Hong L, Turner RT, III, Koelsch G, Shin D, Ghosh AK, Tang J (2002) Crystal structure of memapsin 2 (beta-secretase) in complex with an inhibitor OM00-3. Biochemistry 41:10963–10967.
23. Turner RT, III, Koelsch G, Hong L, Castanheira P, Ermolieff J, Ghosh AK, Tang J, Castenheira P, Ghosh A (2001) Subsite specificity of memapsin 2 (beta-secretase): implications for inhibitor design. Biochemistry 40:10001–10006.
24. Turner RT, III, Hong L, Koelsch G, Ghosh AK, Tang J (2005) Structural locations and functional roles of new subsites S5, S6, and S7 in memapsin 2 (beta-secretase). Biochemistry 44:105–112.
25. Fersht A (1985) Enzyme structure and mechanism. New York: W H Freeman.
26. Riggs L, Seeley EH, Regnier FE (2005) Quantification of phosphoproteins with global internal standard technology. J Chromatogr B Anal Technol Biomed Life Sci 817:89–96.
27. Liu K, Doms RW, Lee VM (2002) Glu11 site cleavage and N-terminally truncated A beta production upon BACE overexpression. Biochemistry 41:3128–3136.
28. Kihara T, Shimmyo Y, Akaike A, Niidome T, Sugimoto H (2010) Abeta-induced BACE-1 cleaves N-terminal sequence of mPGES-2. Biochem Biophys Res Commun 393:728–733.
29. Hartmann T, Bieger SC, Bruhl B, Tienari PJ, Ida N, Allsop D, Roberts GW, Masters CL, Dotti CG, Unsicker K, Beyreuther K (1997) Distinct sites of intracellular production for Alzheimer's disease A beta40/42 amyloid peptides. Nat Med 3:1016–1020.
30. Koo EH, Squazzo SL (1994) Evidence that production and release of amyloid beta-protein involves the endocytic pathway. J Biol Chem 269:17386–17389.
31. Hsiao K, Chapman P, Nilsen S, Eckman C, Harigaya Y, Younkin S, Yang F, Cole G (1996) Correlative memory deficits, Abeta elevation, and amyloid plaques in transgenic mice. Science 274:99–102.
32. Jankowsky JL, Slunt HH, Ratovitski T, Jenkins NA, Copeland NG, Borchelt DR (2001) Co-expression of multiple transgenes in mouse CNS: a comparison of strategies. Biomol Eng 17:157–165.